Laser Shaping for High Brightness Photoelectron Sources

Henry Timmers
The College of Wooster, Wooster, OH 44691, USA
(Dated: August 23, 2007)

It was demonstrated that a 632 nm HeNe laser could be transversely shaped from a Gaussian to flattop beam. The setup used an optical fiber to transmit a circular, single mode beam through a beam expander and into a refractive beam shaper. Once the beam was properly shaped in the transverse domain, a three-lens telescope was used to collimate and image the beam as a means of propagating and demagnifying the beam to a photocathode. This setup will be implemented into the ERL photoinjector and will serve to reduce the emittance of the electron beams.

I. INTRODUCTION

To achieve bright, coherent X-rays from a high energy light source, the emittance of the primary electron beam producing the X-rays must be minimized. One method of minimizing this value is by shaping the laser that excites the electrons from the photocathode in both the transverse and temporal domain. Theoretically, the ideal electron shape that produces linear space charge force is a 3D ellipsoid. For a beam of infinite longitudinal extent, the optimal transverse shape is a flat top. Numerical simulations have been carried out to demonstrate the beam dynamics in the photoinjector under influence of space charge forces. The results show that a uniform laser profile, both in transverse and temporal domains, results in a significantly better performance of the electron source when compared to the unshaped laser distribution.

Furthermore, the optimized laser shape, although different from a flat top in both time and space, has steep edges and can be reasonably well approximated by a uniform 3D cylinder shape [1]. Thus, it was deemed practically feasible to achieve such 3D laser pulse shape as a part of the demonstration of the high brightness electron source being built at Cornell. The research performed this summer was directed towards designing an optical setup to convert a Gaussian laser beam into a flat-top beam using a refractive beam shaper. This optical setup was designed to be implemented into the photoinjector of the Energy Recovery Linac being built in sight of the Cornell Electron Storage Ring.

II. THEORY

A. Emittance

When characterizing an electron beam, the rms emittance can be calculated to quantitatively describe the quality of the beam. The rms emittance measures the parallelism of the beam and can be expressed by the equation

$$\epsilon_r = \sqrt{\langle r^2\rangle\langle p_r^2\rangle - \langle r p_r\rangle^2}, \tag{1}$$

where r represents the radial coordinate and $p_r = \gamma v_r/c$ is a dimensionless momentum component of the axially symmetric beam. The momentum is characterized by γ, the relativistic Lorentz factor, v_r, the radial velocity, and c the speed of light. The brackets describe the central moment of the two quantities and imply a statistical average over all of the electrons in the beam.

The value given by Eq. 1 is the area occupied by a cross-section of the electron beam in phase space. To understand the effects of transverse shaping, the force felt by space charges can be represented by the Lorentz force, or

$$F_r = \frac{eE_r}{\gamma^2}, \tag{2}$$

where E_r is the electric field at the surface of the electron disk and e is the charge of an electron. The radial momentum of the electrons can be found by integrating the Lorentz force over some time Δt, or

$$p_r = \frac{1}{mc}\int_0^{\Delta t} F_r dt \approx \frac{1}{mc}\frac{eE_r}{\gamma^2}\Delta t, \tag{3}$$

where m is the mass of an electron [2].

First, a Gaussian charge distribution is considered for Eq. 3, created when the electrons are excited off the photocathode by a short laser pulse and described by

$$\rho(r) = \rho_o e^{-\frac{r^2}{2\sigma_r^2}}, \tag{4}$$

where ρ_o is the maximum charge density. The Gaussian nature of the beam will result in a momentum that closely resembles $a_1 r + a_3 r^3 + a_5 r^5 + ...$ This non-linearity will produce a non-zero emmitance in the electron beam. A linear momentum function is, theoretically, the only function that will produce a zero emmitance electron beam.

A uniform charge distribution, described by

$$\rho(r) = \begin{cases} \rho_o, & 0 \le r \le R \\ 0, & r > R \end{cases}, \tag{5}$$

can also be considered for the electron beam. The electric field within the area of the beam becomes

$$E_r = \frac{\rho_o}{2\epsilon_o} r, \tag{6}$$

which yields a Lorentz force described by

$$F_r = \frac{e\rho_o}{2\epsilon_o\gamma^2} r. \tag{7}$$

With this force, the radial momentum of the electron disk after a time of Δt becomes

$$p_r = \frac{1}{mc}\int_0^{\Delta t} F_r dt \approx \frac{\rho_o e \Delta t}{2\epsilon_o \gamma^2 mc} r \approx a_1 r. \tag{8}$$

The central moments for r and p_r can then be given by

$$\langle r^2 \rangle = \sigma_r^2, \tag{9}$$

$$\langle p_r^2 \rangle = \langle (a_1 r)^2 \rangle = \langle a_1^2 r^2 \rangle = a_1^2 \sigma_r^2, \tag{10}$$

and

$$\langle r p_r \rangle = \langle a_1 r^2 \rangle = a_1 \sigma_r^2, \tag{11}$$

reducing the beam emittance to

$$\epsilon_r = \sqrt{a_1^2 \sigma_r^4 - (a_1 \sigma_r^2)^2} = 0. \tag{12}$$

Therefore, the emittance growth is minimized by having a transversely uniform electron beam. This is achieved by using a laser with a flattop intensity profile to eject the electrons off the photocathode.

B. Gaussian to Flattop Beam

While various theoretical methods exist to convert a Gaussian laser beam to a flattop profile, the most efficient way is by use of refraction through aspheric lenses. A radially varying magnification can be used to redistribute the light rays to give the desired profile, as shown in Fig. 1.

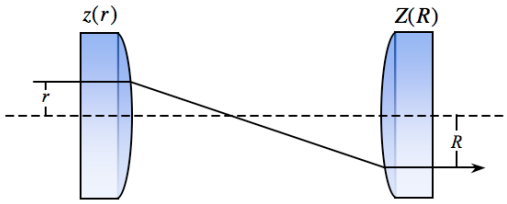

FIG. 1: In the refractive beam shaper, the light rays are redistributed to give a desired output profile.

However, the problem arises of how to manufacture two aspheric lenses to produce a flattop beam. Hoffnagle [3] used an efficient and working method to design his refractive beam shaper. To begin, consider a Gaussian beam with the intensity profile of

$$f(r) = \frac{2}{\pi w_o^2} e^{\frac{-2r^2}{w_o^2}}. \tag{13}$$

It is desired to convert this to some output profile $g[r]$ such that it closely resembles the step function. One particular function that fits this requirement is the Fermi-Dirac function, or

$$g(r) = g_o \left[\frac{1}{1 + e^{\beta\left(\frac{r}{R_o} - 1\right)}}\right], \tag{14}$$

where β determines how rapidly the step function goes from 0 to g_o. During the conversion of $f(r)$ to $g(r)$, it is required that all the power from the beam is to be conserved, therefore

$$\int_0^r f(x) x dx = \int_0^R g(x) x dx, \tag{15}$$

where x is the variable representing the radial distance of a light ray from the axis of propagation, r is the radial distance of the ray at the first aspheric lens, and R is the radial distance of the ray at the second aspheric lens. With this requirement, a relation between the radial distance of the two rays is determined, or $R = h(r)$.

Next, the quantities r and R need to be related with the propagation equations for the light rays at the two aspheric lenses, or $z(r)$ and $Z(R)$. This is achieved by introducing the requirement of a collimated input and output beam as well as Snell's law. To incorporate the prerequisite for collimation mathematically, the optical path difference must remain invariant between the input and output lens.

These requirements lead to a mathematical description of the two lens' surfaces, or

$$z(r) = \int_0^r \left\{(n^2 - 1) + \left[\frac{(n-1)d}{h(x) - x}\right]^2\right\}^{-1/2} dx \tag{16}$$

and

$$Z(R) = \int_0^R \left\{(n^2 - 1) + \left[\frac{(n-1)d}{h^{-1}(x) - x}\right]^2\right\}^{-1/2} dx. \tag{17}$$

III. EXPERIMENT

A. Shaper Instrument

The instrument used to shape the Gaussian beam to flattop was a Refractive Beam Shaper, manufactured by Newport Optics. Newport used the procedure prescribed by Hoffnagle [3] to manufacture the aspheric lens setup. While the design gives an efficient and accurate performance, Eq. 13 and 14, used to describe the input and output profiles, require precise input parameters that makes the experimental conversion rather demanding.

The aspheric lens system was manufactured for a Gaussian input with a waist size of $w_o = 2.366$ mm and a wavelength of $\lambda = 532$ nm, where w_o is defined to be twice the rms beam size. This requires a nearly circular beam with a pristine Gaussian profile and a waste very

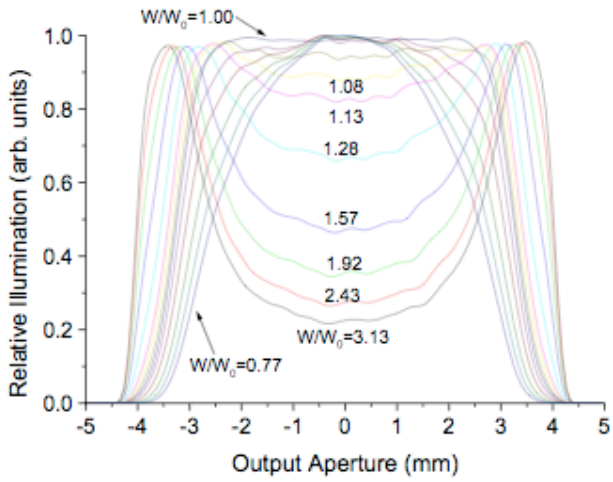

FIG. 2: A plot depicting the effects of waist sizes differing from the ideal value of 2.366 mm [4].

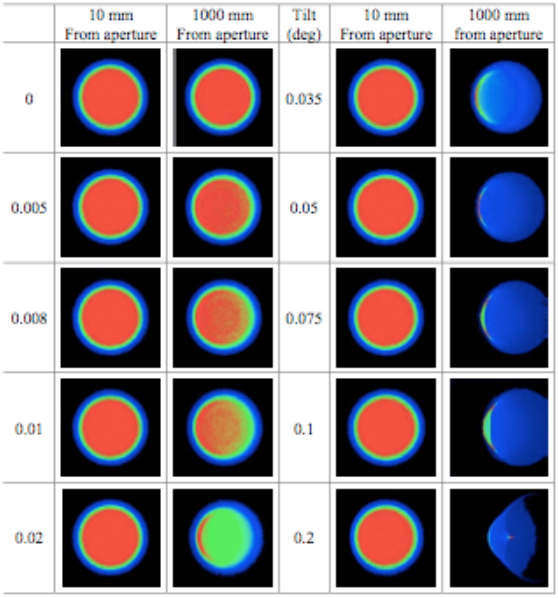

FIG. 3: The profile of the flattop beam for various angular misalignments shown in both the near-field (10 mm) and the far-field (1000 mm) [4].

closely matched to w_o. If the input waist deviates from the accepted input value, the output will deform into a profile differing from a Fermi-Dirac beam, as shown in Fig. 2. If the input waist is greater than w_o, the profile will begin to grow "cat ears" in which the outer edge of the beam peaks in intensity. When the input waist is less than w_o, the profile will resemble a flattened Gaussian in which the profile is still curved, but there is far less curvature [4].

Another important prerequisite for the refractive shaper is a high quality laser beam determined by the ellipticity and the beam propagation factor, or M^2. The value of M^2 should be less than 1.1 while the beam ellipticity, defined as a ratio of major and minor axes, should be 0.95 or better. One final requirement is that the laser beam should go precisely perpendicular through the beam shaper. Any minor angular or translational misalignments will cause deformities in the flattop beam down the propagation axis. The far-field deformities are dominated by angular misalignments and even an error of 0.2° will greatly distort the beam 1.00 m down the line, as shown in Fig. 3 [4].

B. Initial Setup

The laser used in the initial setup was a TECGL-05 532 nm diode laser with a power output of 5 mW and manufactured by World Star Tech. The laser was approximately 10 % elliptical and had a waist size of $w_o \approx 0.45$ mm. To achieve the correct input radius, a three lens telescope was setup and ray tracing matrices were used to determine the focal lengths and distances for the telescope. The final matrix is given in Eq. 18 and solving elements $M_{21} = 0$ and $M_{11} = 2.366\ \text{mm}/w_o$ gave solutions that guaranteed that the beam would be both collimated and magnified to the correct spot size.

$$M = \begin{pmatrix} 1 - \frac{d_2+d_1\left(1+\frac{d_2}{f_2}\right)}{f_1} + \frac{d_2}{f_2} & d_2 + d_1\left(1+\frac{d_2}{f_2}\right) \\ \frac{(f_1-d_1)(f_1-d_2)+f_2(d_1+d_2-2f_1)}{f_1^2 f_2} & 1 - \frac{d_2+d_1}{f_1} + \frac{d_1(1-\frac{d_2}{f_1})}{f_2} \end{pmatrix} \tag{18}$$

Once the correct radius was achieved, the beam was directed into the refractive beam shaper. To allow for precise alignment, a multi-directional stage was setup that allowed adjustment in the x-axis, y-axis, z-axis, and the two angular axes (pitch and yaw). The x, y, and z axes were adjusted in the near-field using a note card to determine the beam quality and making sure the beam was perfectly centered through the aspheric lenses. The pitch

and yaw were then adjusted in the far-field using the wall approximately 3 m away from the shaper to look at the beam's quality.

Finally, the beam was imaged using a CCD camera to look at the 2-dimensional intensity profile and make final adjustments in the mount axes. Reflective filters were used to attenuate the beam into the Spiricon CCD camera. The beam was attenuated until the CCD fell just short of saturation in order to use the full dynamic range of the detector. This setup can be seen in Fig. 4. Occasionally, the filters were placed in front of the telescope to minimize the development of fringe patterns on the CCD.

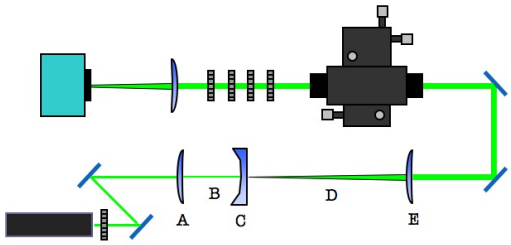

FIG. 4: The initial setup in which the laser went through a beam expander and then into the refractive beam shaper.

After many futile attempts to achieve a high quality flattop beam with this setup, it was realized that the beam from the 532 nm laser diode was not up to par with the stern requirements of the beam shaper. The best value for the roundness of the beam was 0.799 after the beam expander, shown in Fig. 5 *a*. The corresponding output would consistently give a profile as depicted in Fig. 5 *b*, in which the major axis would have a "cat ear" profile while the minor axis would have a cut-off, flattened Gaussian. The problem was traced to poor ellipticity of the laser, which was confirmed by rotating the laser by 90° and observing the corresponding rotation of the shape on the CCD.

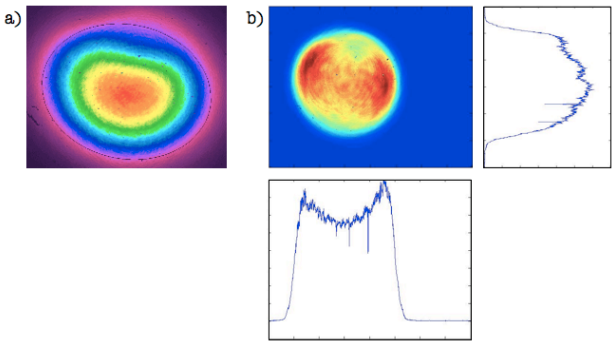

FIG. 5: a) The input of the beam shaper using the diode laser with a $w_o = 2.368$ mm and a roundness of 0.799 with b) the corresponding output of the shaper.

C. Beam Quality Measurement

To verify that the deformity in Fig. 5 *b* was an artifact of the 532 nm diode laser, the beam quality factor was measured for both the horizontal and vertical planes. The beam quality factor, or M^2, is a measure of the focusability of the laser beam. Since the beam is influenced by diffraction, it cannot be focused to a single point. The measure by which the beam parameter product, which is a product of a lasers beam angle and radius at the location of the beam waist, deviates from the diffraction limit is determined by the value of M^2. Ideally, this quantity should be one, however, factors such as ellipticity and the number of modes present affect the M^2 value.

M^2 was measured by focusing the laser with a $f = 200$ mm lens. The 4σ diameter, for both the major and minor axes, was recorded for 20 data points about two Rayleigh lengths of the smallest beam waist. One Rayleigh length was defined to be the distance it took for the area of the beam to double [5]. The results gave a set of data with which a hyperbola could be fit to, or

$$d[z] = \sqrt{a + bz + cz^2}, \tag{19}$$

where $d[z]$ is the diameter of the beam and z is the propagation distance from the focusing lens. The beam quality factor could then be found with

$$M^2 = \frac{\pi}{8\lambda}\sqrt{4ac - b^2}. \tag{20}$$

The 532 nm diode beam yielded two different beam quality factors of $M_x^2 = 1.40$ and $M_y^2 = 1.04$ for the major and minor axes respectively. The data and fit hyperbola for the two axes is shown in Fig. 6. The first important conclusion was that the two quantities differ by 25.7 %. This means that the two axes are diverging at different rates which explains why the beam becomes more elliptical as it travels through the beam expander. The other conclusion was that, as previously stated, the beam shaper requires beams with $M^2 < 1.1$ which means a new laser would have to be used.

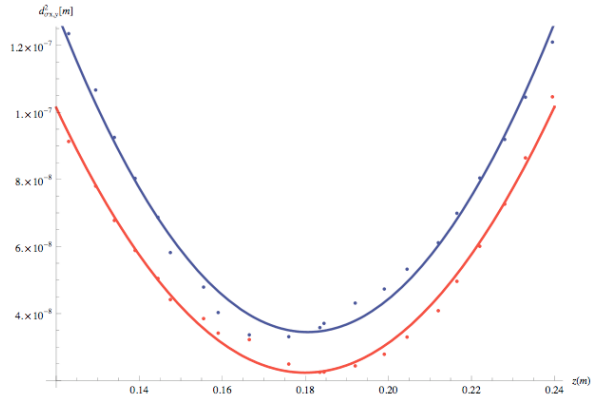

FIG. 6: A plot of the beam diameter squared vs. propagation distance, used to find a value for M^2.

D. Fiber Optic Setup

Most lasers are not manufactured to have low ellipticity, therefore it was decided to design a new setup in which an optical fiber was used to clean up the quality of a 632 nm HeNe laser beam. In the new setup, the beam was first passed through a set of reflective filters so it could be imaged with a CCD down the line. It was then guided into a 10x objective which focused it down to where it could be captured by a SM600 optical fiber 5 mm away. This fiber was a single mode fiber with a diameter of 4.45 μm and an NA = 0.12. The ability of the fiber to pass only the single, fundamental mode of the beam would serve to reduce the M^2 of the beam as well as give it a circular profile.

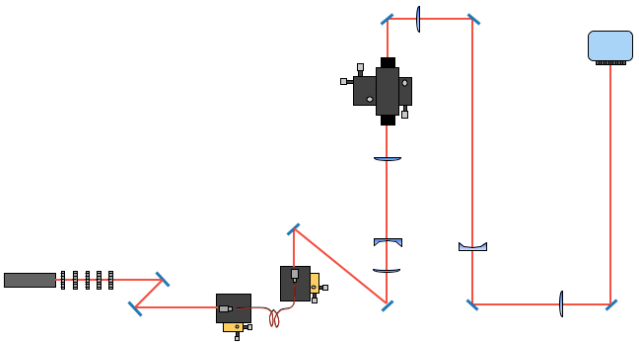

FIG. 7: The final setup of the project which used an optical fiber to clean up the input into the shaper.

As the beam exited the fiber, it was captured by another 10x objective 5 mm away which served to collimate the beam. The beam width, at this point, was initially measured in order to determine the distances within the beam expander. The beam was then passed through the beam expander to give it a radius of 2.366 mm. This setup proved to be a success, yielding an almost perfect flattop beam as shown in Fig. 8. After the expander, the collimated beam was sent through the refractive beam shaper and the same procedures described above were used to align the beam in the shaper in both the near and far field. Once the beam was shaped and properly aligned, it was passed through an optical system which demagnified it by a factor of three (or six) and was imaged using a CCD camera. The whole setup is shown in Fig. 7.

E. Demagnification Problem

The ERL photogun not only requires a flattop laser beam to perform with low emittance, it also needs to have a particular size at the photocathode, which is smaller than the output beam from the commercially available shaper that was used. Depending on various parameters, such as the gun voltage and charge in a single bunch, the beam width will have to be demagnified by up to a

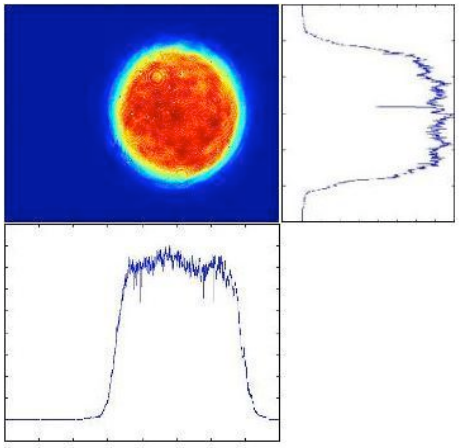

FIG. 8: The output of the shaper with the Fiber Optic setup.

factor of six. Whereas, conceptually, this does not pose any challenge, in practice, there are two obstacles that can make it rather difficult. First, the minimum distance the beam would have to propagate from the last optical element in order to reach the photocathode was roughly 1.5 m. At the same time, the flattop profile would begin degrading in quality after one meter. Second, the beam also had to pass a small in-vacuum mirror, about 10.77 mm wide, used to guide the beam to the photocathode. Making a larger mirror would involve changing the vacuum chamber structure of the light box that couples the laser beam into the ultra-high vacuum (UHV) environment, as well as modifying several electron beamline components upstream. Therefore, if possible, the beam had to be less than 10 mm in diameter at a distance of about 560 mm from the last optical element in order not to clip the flattop beam.

Many types of imaging and telescope systems were experimented with in an attempt to fulfill the conditions of the electron gun. They are summed up in Table I. The first setup that was tried was a complex telescope which was meant to collimate and demagnify the beam. The negative focal lens had a large f-number which actually worked to redistribute the flattop rays back to a Gaussian profile.

To insure that it was indeed the negative focal length lens that was distorting the beam profile, a unity Keplerian telescope was constructed. The performance of this telescope was observed through a propagation range of 200-2750 mm. The problematic negative focal length lens was then placed into the telescope at the focal length of the first lens to maintain unity magnification. Theoretically, the output of the telescope should remain the same, however, the lens brought out a different mode of the laser characterized by concentric rings of intensity.

Next, a simple Keplerian design was used to demagnify the beam since the previous, unity telescope had worked fairly well. However, since the ray angles scale by the in-

TABLE I: A table of the main optical systems experimented with to relay the flattop beam to the photocathode. The distances and focal lengths are in sequential order to where they appear in the setup.

Telescope Type	Magnification	d_1 (mm)	f_1 (mm)	d_2 (mm)	f_2 (mm)	d_3 (mm)	f_3 (mm)	d_4 (mm)
Complex	1/6	750	300	265	-30	90	300	varied
Kepelerian	-1	320	300	600	300	varied	–	–
Complex	-1	320	300	300	-30	300	300	varied
Kepelerian	-1/3	320	300	400	300	varied	–	–
Imaging	-0.355	100	1000	941.9	-200	581.9	500	1500

verse of magnification [4], any minor discrepancies would be magnified by this setup. As a result, the output of the telescope looked more like a tapered Gaussian than a flattop.

The final system tested used a three-lens telescope to both image and collimate the beam. The magnification and imaging distance (the distance from the last lens to the imaging plane) were both theoretically set to $m = -0.355$ and $d_4 = 1.5$ m to fulfill the space requirements imposed by the electron gun and beamline geometry. This setup relayed the beam nearly perfect, as shown in Fig. 9, with an actual magnification of $|m| = 0.381$.

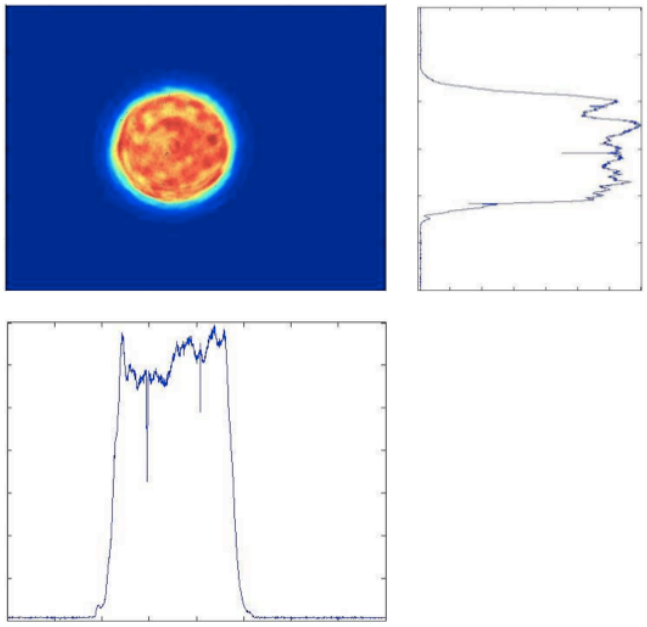

FIG. 9: The output of the imaging telescope used to demagnify and propagate the beam.

IV. APPLICATION AND CONCLUSION

While the actual setup for the ERL photoinjector required a demagnification by a factor of six, the final telescope setup worked to demonstrate that the flattop beam could be both imaged and collimated to a large distance away. The magnification factor only varied by 7% from what it was theoretically set to be and the beam would remain flattop to a distance of plus or minus a few cm from the final imaging distance. Future work could be directed towards designing an imaging telescope that, not only demagnifies by a factor of up to six, but also has distances that could be reasonably implemented into the electron gun.

With the meticulous alignment and the excellent performance of the Refractive beam shaper demonstrated, work can begin on characterizing and designing the optical setup necessary for the actual laser system to be used with the gun. This laser will be implemented into the final setup of the ERL photoinjector, and the use of the imaging telescope will allow the flattop beam to imaged onto the photocathode with an optimal size, and create a low emittance, bright electron beam.

V. ACKNOWLEDGMENTS

Many thanks to Ivan Bazarov for his guidance and support throughout the summer, as well as the ERL laser group, consisting of Frank Wise, Bruce Dunham, Dimitre Ouzounov, and Heng Li, for their continual advising and support. Thanks also to Rich Galik, Monica Wesley, and Peggy Steenrod for establishing and maintaining the LEPP REU program at Cornell University. This work was supported by the National Science Foundation REU grant PHY-0552386 and research co-operative PHY-0202078.

[1] I.V. Bazarov, C.K. Sinclair, "Multivariate optimization of a high brightness dc gun photoinjector", Physical Review Special Topics: Accelerator Beam, Vol. 8, 034202 (2005)

[2] Y. E. Sun, K. J. Kim, P. Piot, "Effects on Flat-Beam Generation From Space-Charge Force and Beamline Errors," *Proceedings PAC 2005*, 3774-3776 (2005).

[3] J. A. Hoffnagle and C. M. Jefferson, "Design and performance of a refractive optical system that converts a Gaussian to a flattop beam," *Applied Optics*, **39**, 5488-5499 (2000).

[4] J. A. Hoffnagle and C. M. Jefferson, "Ashperic Laser Beam Reshaper Applications Guide," *IBM Almaden Research Center*.

[5] *Test methods for laser beam widths, divergence angles and beam propagation ratios – Part 1: Stigmatic and simple astigmatic beams*, Document ISO 11146-1, International Organization for Standardization (Jan. 2005).